Simplified Soft-Output Demapper for Binary Interleaved COFDM with Application to HIPERLAN/2

Filippo Tosato[1], Paola Bisaglia
Imaging Systems Laboratory
HP Laboratories Bristol
HPL-2001-246
October 10th , 2001*

In this paper a comparison in performance between hard and soft decision Viterbi decoding, with application to the HIPERLAN/2 standard, is presented. The results show that when channel state information (CSI) is included in the generation of the soft decision information, the soft decision method greatly outperforms the hard method. Moreover, a simplified algorithm for the soft-output demapper for the 16-QAM and 64-QAM constellations is developed, which allows the complexity of the demapper to be maintained at almost the same level for all the possible modes of HIPERLAN/2.

Simplified Soft-Output Demapper for Binary Interleaved COFDM with Application to HIPERLAN/2

Filippo Tosato[1] and Paola Bisaglia[2]

[1] Dipartimento di Elettronica e Informatica, University of Padova, Via Gradenigo 6/A, 35131 Padova, Italy
[2] Hewlett–Packard Laboratories, Filton Road, Stoke Gifford, Bristol BS34 8QZ, U.K.

Abstract— **In this paper a comparison in performance between hard and soft decision Viterbi decoding, with application to the HIPERLAN/2 standard, is presented. The results show that when channel state information (CSI) is included in the generation of the soft decision information, the soft decision method greatly outperforms the hard method. Moreover, a simplified algorithm for the soft-output demapper for the 16-QAM and 64-QAM constellations is developed, which allows the complexity of the demapper to be maintained at almost the same level for all the possible modes of HIPERLAN/2.**

I. INTRODUCTION

HIPERLAN/2, the European standard recently specified by ETSI BRAN, has been designed to provide several data rates, selected according to the channel conditions, for short-range communications in indoor and outdoor environments. OFDM has been chosen as the modulation format because of its good performance in highly dispersive channels. The data rate ranging from 6 Mbit/s to 54 Mbit/s, can be varied by using various signal alphabets for modulating the OFDM sub–carriers and by applying different puncturing patterns to a mother convolutional code. BPSK, QPSK and 16-QAM are used as mandatory modulation formats, whereas 64-QAM is optional [1].

Previous results on HIPERLAN/2 have suggested the use of a hard decision Viterbi decoder for decoding the convolutional code, while the soft decision Viterbi decoder has not been considered because of its greater computational complexity, especially when higher modulation formats are employed. In fact, in the case of the 16-QAM and 64-QAM constellations, each axis carries more than one bit and the metric functions, in the soft-output demapper, to determine the soft information for each bit, are in general quite complicated. Instead, in the case of BPSK and QPSK, the soft information is simply proportional to the distance from the decision boundary.

In this paper, after reviewing two different approaches of implementing the soft-output demapper and soft-input Viterbi decoder for multi-level modulations, we adapt the Pyndiah's algorithm [2] to COFDM systems and propose a simplified version of it which allows us to reduce the complexity in the case of higher order constellations.

Simulation results show that in a typical HIPERLAN/2 channel a significant improvement in performance is obtained using soft decision decoding compared to hard-decision decoding.

The structure of this paper is as follows. In Section II the HIPERLAN/2 system model is introduced, in Section III two soft decoding schemes with bit metric calculation and soft bit information are described and compared, in Section IV a simplified soft bit computation is proposed. Finally, in Section V some numerical results are presented on the performance of HIPERLAN/2 with the proposed low complexity soft Viterbi decoding.

II. SYSTEM MODEL

In Figure 1 the HIPERLAN/2 system model on which we base our analysis is shown. At the transmitter, the input bits, after scrambling, are convolutionally encoded with a rate 1/2, constraint length 7 convolutional code[1], bit-by-bit interleaved and then converted into QAM symbols, according to Gray-coded constellation mappings. This scheme is also called Bit-Interleaved Coded Modulation (BICM) [3]. The complex symbols are then fed to an OFDM modulator, arranged into a physical frame called physical (PHY) burst with an appropriate preamble, and finally transmitted.

Let $M = 2^{2m}$ be the number of symbols of the generic square QAM constellation, so that m interleaved bits are mapped into the in-phase and quadrature components of the complex symbol[2]. Let $a[i] = a_I[i] + ja_Q[i]$ denote the QAM symbol transmitted in the i-th sub-carrier and $\{b_{I,1}, \ldots, b_{I,k}, \ldots, b_{I,m}, b_{Q,1}, \ldots, b_{Q,k}, \ldots, b_{Q,m}\}$ the corresponding bit sequence. Assuming that the cyclic prefix completely eliminates ISI (Inter OFDM Symbol Interference) and ICI (Inter Channel Interference), then the received signal in the generic sub-carrier can be written as

$$r[i] = G_{ch}(i) \cdot a[i] + w[i] \,, \qquad (1)$$

where $G_{ch}(i)$ is the Channel Frequency Response (CFR) complex coefficient in the i-th sub-carrier and $w[i]$ is the complex AWGN noise with variance $\sigma^2 = N_0$.

At the receiver, the OFDM demodulator performs synchronization and channel estimation, the latter being used by a zero-forcing equalizer which compensates for attenuation and phase shift in each data sub-carrier. If the channel estimate is error free, the output of the one-tap equalizer is given by

---

[1] Two different puncturing patterns can be applied to obtain code rates 3/4 and 9/16 [1].
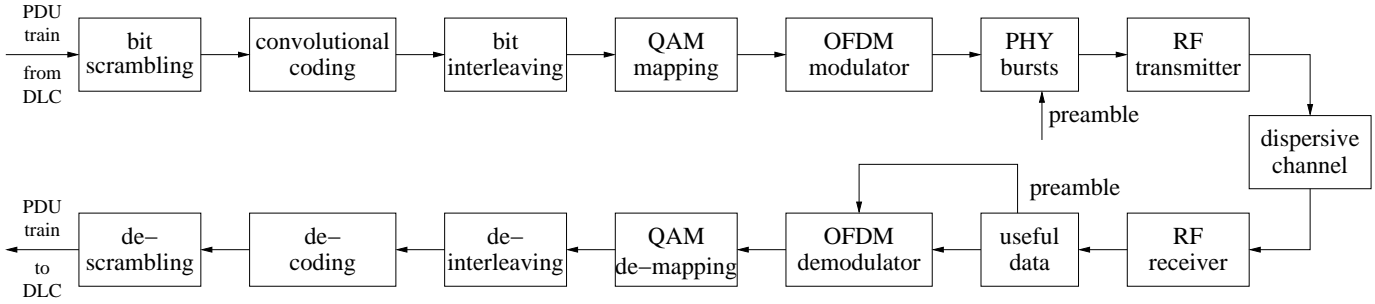[2] For BPSK only the in-phase component is present.

Fig. 1. Block diagram of HIPERLAN/2 PHY layer.

$$y[i] = a[i] + w[i]/G_{ch}(i) = a[i] + w'[i] , \qquad (2)$$

where $w'[i]$ is still complex AWGN noise with variance $\sigma'^2(i) = \sigma^2/|G_{ch}(i)|^2$.

III. Soft Maximum Likelihood Decoding for Binary Interleaved Coded Modulation

Soft Viterbi decoding for BICM employing BPSK or QPSK modulations is straightforward as the soft bit information, before being weighted by the CSI coefficients, is simply given by the received signals for BPSK and by their in-phase and quadrature components for QPSK. Therefore in the following discussion we will focus on the higher modulation levels, namely 16- and 64-QAM.

A. ML bit metrics

Because interleaving is applied to the encoded bits before the QAM modulator, Maximum Likelihood Decoding (MLD) of multi-level BICM signals would require joint demodulation and convolutional decoding and is therefore quite complex to implement in practice [4]. In fact, according to the MAPSE (Maximum A Posteriori Sequence Estimation) criterion the following maximization should be performed to estimate the encoded bit sequence $\mathbf{b}$:

$$\widehat{\mathbf{b}} = \arg\max_{\mathbf{b}} P[\mathbf{b}|\mathbf{r}] , \qquad (3)$$

where $\mathbf{r}$ is the received sequence of QAM signals. We also assume that perfect CSI is available, i.e. $\{G_{ch}(i)\}$ are known to the receiver. Thus, all possible coded and interleaved bit sequences would have to be considered for (3) to be evaluated. In [5], Zehavi proposed a decoding scheme which consists in calculating sub-optimal simplified bit metrics to be used inside a Viterbi decoder for path metric computation. For each symbol $r[i]$, $4m$ metrics need to be derived, two for each in-phase and quadrature bit $b_{I,k}$, $b_{Q,k}$, corresponding to possible values $0, 1$. For bit $b_{I,k}$ (the same applies to bit $b_{Q,k}$) first the QAM constellation is split into two partitions of complex symbols, namely $S_{I,k}^{(0)}$ comprising the symbols with a '0' in position (I,k) and $S_{I,k}^{(1)}$ which is complementary. Then the two metrics are obtained by

$$m'_c(b_{I,k}) = \max_{\alpha \in S_{I,k}^{(c)}} \log p(r[i] \mid a[i] = \alpha) , \ c = 0, 1 . \quad (4)$$

Since the conditional pdf of $r[i]$ is complex Gaussian

$$p(r[i] \mid a[i] = \alpha) = \frac{1}{\sqrt{2\pi}\sigma} \exp\left\{-\frac{1}{2}\frac{|r[i] - G_{ch}(i)\,\alpha|^2}{\sigma^2}\right\} , \qquad (5)$$

and as $r[i] = G_{ch}(i) \cdot y[i]$, the metrics (4) are equivalent to

$$m_c(b_{I,k}) = |G_{ch}(i)|^2 \cdot \min_{\alpha \in S_{I,k}^{(c)}} |y[i] - \alpha|^2 \ , \quad c = 0, 1 . \quad (6)$$

Finally, these metrics are de-interleaved, i.e. each couple (m_0, m_1) is assigned to the bit position in the decoded sequence according to the de-interleaver map, and fed to the Viterbi decoder which selects the binary sequence with the smallest cumulative sum of metrics.

B. LLR soft bit values

BICM allows a different MAPSE-based decoding scheme in which the received QAM signals are first demodulated by a *soft-output demapper* and de-interleaved, and then passed to a standard *binary soft-input Viterbi decoder* [6]. The idea is to demap the received signal into soft bits which have the same sign as provided by a hard detector and whose absolute value indicates the reliability of the decision.

The optimum hard decision on bit $b_{I,k}$ (the same applies for bit $b_{Q,k}$) is given by the rule

$$\widehat{b}_{I,k} = \beta \ \text{ if } \ P[b_{I,k} = \beta \mid r[i]] > P[b_{I,k} = (1 - \beta) \mid r[i]] \ ,$$
$$\beta = 0, 1 . \quad (7)$$

Set $\beta = 1$, then (7) can be rewritten as

$$\widehat{b}_{I,k} = 1 \quad \text{if} \quad \log\frac{P[b_{I,k} = 1 \mid r[i]]}{P[b_{I,k} = 0 \mid r[i]]} > 0 . \qquad (8)$$

Thus, the Log-Likelihood Ratio (LLR) of decision $\widehat{b}_{I,k}$ is defined as[3]

$$LLR(b_{I,k}) = \log\frac{P[b_{I,k} = 1 \mid r[i]]}{P[b_{I,k} = 0 \mid r[i]]}$$
$$= \log\frac{\sum_{\alpha \in S_{I,k}^{(1)}} P[a[i] = \alpha \mid r[i]]}{\sum_{\alpha \in S_{I,k}^{(0)}} P[a[i] = \alpha \mid r[i]]} , \qquad (9)$$

[3]If we set $\beta = 0$ in (7), then the LLR function shall be defined with the opposite sign.

which is the soft bit information assigned to bit $b_{I,k}$.

By applying Bayes rule and assuming that the transmitted symbols are equally distributed, relation (9) yields

$$LLR(b_{I,k}) = \log \frac{\sum_{\alpha \,\in\, S_{I,k}^{(1)}} p\left(r[i] \mid a[i] = \alpha\right)}{\sum_{\alpha \,\in\, S_{I,k}^{(0)}} p\left(r[i] \mid a[i] = \alpha\right)} \; . \qquad (10)$$

Sub-optimal simplified LLR can be obtained by the log-sum approximation: $\log \sum_j z_j \approx \max_j \log z_j$, which is good as long as the sum in the left-hand side is dominated by the largest term, as typically occurs in channels with high Signal-to-Noise Ratio (SNR). Thus

$$LLR(b_{I,k}) \approx \log \frac{\max_{\alpha \,\in\, S_{I,k}^{(1)}} p\left(r[i] \mid a[i] = \alpha\right)}{\max_{\alpha \,\in\, S_{I,k}^{(0)}} p\left(r[i] \mid a[i] = \alpha\right)} \; . \qquad (11)$$

Using (5) in (11) and normalizing by $2/\sigma^2$ the final soft bit values can be calculated as:

$$LLR(b_{I,k}) =$$
$$= \frac{|G_{ch}(i)|^2}{4} \left\{ \min_{\alpha \,\in\, S_{I,k}^{(0)}} |y[i] - \alpha|^2 - \min_{\alpha \,\in\, S_{I,k}^{(1)}} |y[i] - \alpha|^2 \right\}$$
$$= [m_0(b_{I,k}) - m_1(b_{I,k})]/4 \; . \qquad (12)$$

In the Appendix we demonstrate that using the approximate bit metrics (6) for path metric calculation inside the Viterbi Algorithm (VA) is equivalent to demodulating the received signals into soft bit values according to (12) and then employing a soft binary VA for decoding.

Yet, expression (12) allows further simplification with significant reduction of computational complexity and negligible soft decoding performance loss. Moreover, with the second scheme the same standard implementation of soft-input Viterbi decoder for BPSK signals can be used also for multi-level modulations.

IV. Simplified LLR computation

Figure 2 shows the partitions $(S_{I,k}^{(0)}, S_{I,k}^{(1)})$ for the generic bit $b_{I,k}$, and $(S_{Q,k}^{(0)}, S_{Q,k}^{(1)})$ for the bit $b_{Q,k}$, in the case of the 16-QAM constellation. As can be seen they are delimited by either horizontal or vertical boundaries. Therefore, the two symbols within the two subsets, nearest to the received equalized signal, always lie in the same row if the partition boundaries are vertical (bits $b_{I,1}$ and $b_{I,2}$ in Figure 2) or in the same column if the boundaries are horizontal (bits $b_{Q,1}$ and $b_{Q,2}$ in Figure 2). The same observation holds true for the 64-QAM constellation. As a consequence, equation (12) can be rewritten as:

$$LLR(b_{I,k}) =$$
$$= \frac{|G_{ch}(i)|^2}{4} \left\{ \min_{\alpha_I \,\in\, S'^{(0)}_{I,k}} (y_I[i] - \alpha_I)^2 - \min_{\alpha_I \,\in\, S'^{(1)}_{I,k}} (y_I[i] - \alpha_I)^2 \right\}$$
$$\triangleq |G_{ch}(i)|^2 \cdot D_{I,k} \; , \qquad (13)$$

where subset $S'^{(c)}_{I,k}$ contains the real parts of the complex symbols of subset $S_{I,k}^{(c)}$, for $c = 0, 1$.
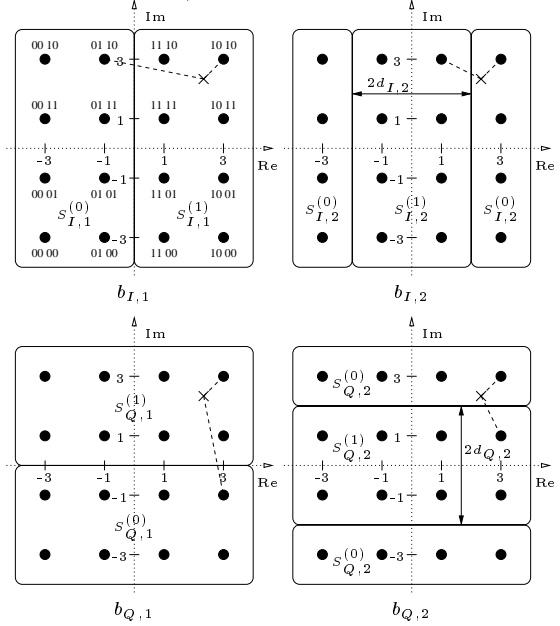

Fig. 2. Partitions of the 16-QAM constellation used in HIPERLAN/2 PHY layer.

Evaluation of the terms $D_{I,k}$ for the in-phase bits of a 16-QAM symbol yields

$$D_{I,1} = \begin{cases} y_I[i] \,, & |y_I[i]| \le 2 \\ 2(y_I[i] - 1) \,, & y_I[i] > 2 \\ 2(y_I[i] + 1) \,, & y_I[i] < -2 \end{cases} \qquad (14)$$

$$D_{I,2} = -|y_I[i]| + 2 \; . \qquad (15)$$

It can be easily verified that the $D_{Q,k}$ functions for the two quadrature bits are the same as (14) and (15) with $y_I[i]$ replaced by $y_Q[i]$.

Similarly, formulas can be derived from (13) for the in-phase bits of the 64-QAM constellation:

$$D_{I,1} = \begin{cases} y_I[i] \,, & |y_I[i]| \le 2 \\ 2(y_I[i] - 1) \,, & 2 < y_I[i] \le 4 \\ 3(y_I[i] - 2) \,, & 4 < y_I[i] \le 6 \\ 4(y_I[i] - 3) \,, & y_I[i] > 6 \\ 2(y_I[i] + 1) \,, & -4 \le y_I[i] < -2 \\ 3(y_I[i] + 2) \,, & -6 \le y_I[i] < -4 \\ 4(y_I[i] + 3) \,, & y_I[i] < -6 \end{cases} \qquad (16)$$

$$D_{I,2} = \begin{cases} 2(-|y_I[i]| + 3) \,, & |y_I[i]| \le 2 \\ 4 - |y_I[i]| \,, & 2 < |y_I[i]| \le 6 \\ 2(-|y_I[i]| + 5) \,, & |y_I[i]| > 6 \end{cases} \qquad (17)$$

$$D_{I,3} = \begin{cases} |y_I[i]| - 2 \,, & |y_I[i]| \le 4 \\ -|y_I[i]| + 6 \,, & |y_I[i]| > 4 \end{cases} . \qquad (18)$$

Expressions (14)-(15) are similar to the LLR functions for bit reliability derived by Pyndiah in [2], in the case of a single carrier system over a Gaussian channel and applied to near optimum decoding of product codes. However, unlike a single carrier system in which all data symbols are affected by the same SNR on average, in a multi-carrier OFDM system the various carriers suffer from different channel attenuation levels and so data conveyed by sub-carriers having a high SNR are *a priori* more reliable than those transmitted in sub-carriers with low SNR. This additional information is supplied to the decoder by weighting the LLR functions by the square modulus of the CFR, which represents the Channel State Information (CSI), as can be seen in (12). Note also that the CSI coefficient is proportional to the SNR in the i-th sub-channel:

$$\text{SNR}_i \propto |G_{ch}(i)|^2 \ . \tag{19}$$

Expressions (14) and (16)-(17) are still cumbersome to evaluate, so we introduce a further simplification. Expression (14) can be approximated as follows:

$$D_{I,1} \simeq y_I[i] \ , \tag{20}$$

and the same applies to the first quadrature bit.

The approximate expressions for (16)-(18) are given by

$$D_{I,1} \simeq y_I[i] \tag{21}$$
$$D_{I,2} \simeq -|y_I[i]| + 4 \tag{22}$$
$$D_{I,3} = -||y_I[i]| - 4| + 2 \ . \tag{23}$$

These approximations correspond to calculating $|D_{I,k}|$ (or $|D_{Q,k}|$) as the distance of the received equalized signal $y[i]$ from the nearest partition boundary and assigning to $D_{I,k}$ (or $D_{Q,k}$) the sign + or - according to which partition $y[i]$ falls in.

In Figures 3 and 4, the approximate functions are plotted versus the theoretical ones for both 16- and 64-QAM.
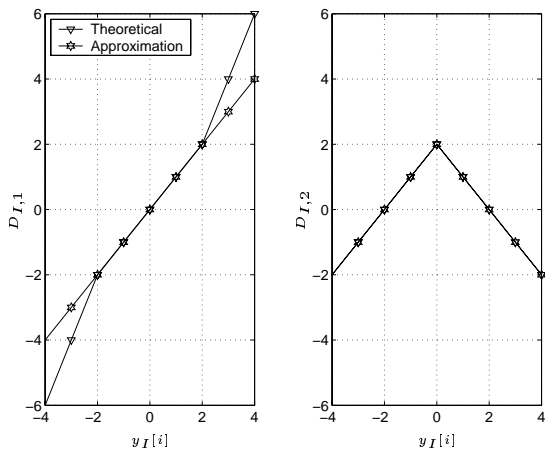

Fig. 3. Approximate versus exact LLR functions for the in-phase bits of the 16-QAM constellation of Figure 2.

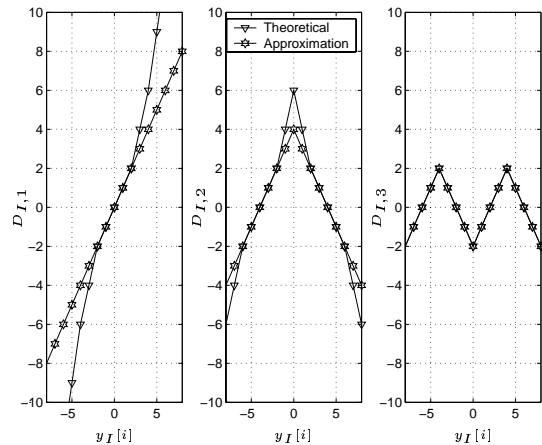Formulas (20) and (15), and (21)-(23) can be generalized for any square QAM constellation with similar Gray

Fig. 4. Approximate versus exact LLR functions for the in-phase bits of the 64-QAM constellation.

labelling[4]. Let $d_{I,k}$ and $d_{Q,k}$ denote half the distance between the partition boundaries relative to bit $b_{I,k}$ and $b_{Q,k}$, with $k > 1$ (see Figure 2). Then, the LLR functions can be approximated as:

$$D_{I,k} \simeq \begin{cases} y_I[i] \ , & k = 1 \\ -|D_{I,k-1}| + d_{I,k} \ , & k > 1 \end{cases} \tag{24}$$

$$LLR(b_{I,k}) = |G_{ch}(i)|^2 \cdot D_{I,k} \quad , \quad k \geq 1 \ ,$$

and

$$D_{Q,k} \simeq \begin{cases} y_Q[i] \ , & k = 1 \\ -|D_{Q,k-1}| + d_{Q,k} \ , & k > 1 \end{cases} \tag{25}$$

$$LLR(b_{Q,k}) = |G_{ch}(i)|^2 \cdot D_{Q,k} \quad , \quad k \geq 1 \ .$$

Note that $d_{I,k} = d_{Q,k}$ for all k, for the Gray labelling we have considered.

V. Numerical results

The results, obtained by computer simulations, are given in terms of Bit Error Rate (BER) versus E_b/N_0, where E_b is the energy per information bit. In order to verify the performance of the hard and soft decoding for the four possible modulation formats, modes $1, 4, 5$ and 7 of HIPERLAN/2, using BPSK, QPSK, 16-QAM and 64-QAM, respectively, have been employed. We note however that similar results should be expected with the other modes since they only differ in the puncturing schemes; moreover from [7], mode 2 and mode 3 should perform as mode 4 and mode 1, respectively. The curves have been generated averaging over 2000 different realizations of channel model A [7], typical for large office environment with non-line-of sight propagation. In all cases, the decision depth in the Viterbi decoder has been fixed to 60.

Results for mode 1 (continuous line) and mode 4 (dashed line) in Figure 5 show that at a BER $= 10^{-4}$ the soft-decoding gain compared to hard-decoding is equal to 4.5 dB and 6.5 dB, respectively. In Figure 6, where mode 5 (continuous line) and mode 7 (dashed line) are used, the

---

[4]For other Gray labelling patterns only minor changes are needed.

gain of the soft-decoding compared to hard-decoding is equal to 6.5 dB and 8.5 dB, respectively, at a BER of 10^{-4}. As it can be observed from Figure 6, in both cases of the 16-QAM and 64-QAM constellations, there is no performance degradation from the theoretical formulas given in (14)-(15) and (16)-(18), using our proposed approximated formulas in (24)-(25); therefore the latter can be used with a reduction in computational complexity.
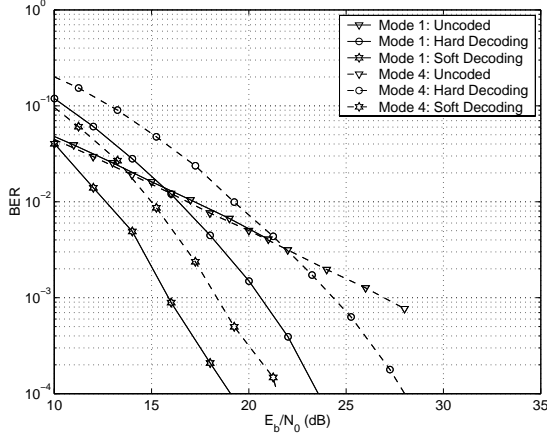

Fig. 5. Comparison between hard and soft decoding for mode 1 and mode 4 of HIPERLAN/2, with channel model A.
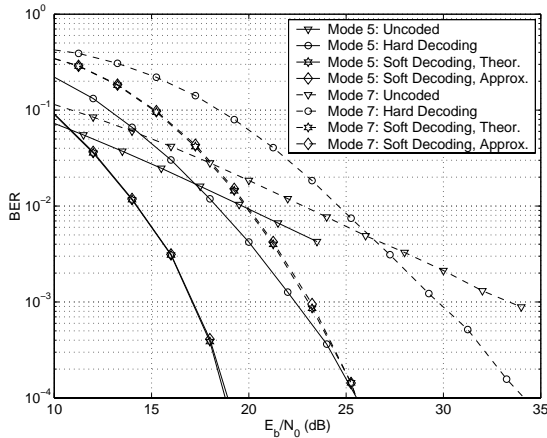

Fig. 6. Comparison between hard and soft decoding with exact and approximated computation of soft bit values for mode 5 and mode 7 of HIPERLAN/2, with channel model A.

VI. CONCLUSIONS

In this paper we have presented some new results on the performance of HIPERLAN/2 transmission modes with soft Viterbi decoding. We have adopted a decoding scheme in which the received complex symbols are demapped into soft bit information which is weighted by the CSI coefficients and then fed to a conventional soft binary Viterbi decoder. This scheme is equivalent to that proposed by Zehavi for BICM, requiring soft metric calculation. Simplified formulas for the LLR computation have been proposed which show no performance loss compared to the theoretical ones. Gains from 4.5 dB (for mode 1) up to 8.5 dB (for mode 7), at BER = 10^{-4} have been obtained over hard decoding.

APPENDIX

EQUIVALENCE BETWEEN SOFT DECODING SCHEMES WITH BIT METRICS (6) AND SOFT BITS (12)

We indicate the soft decoding scheme with bit metric generation (6) and Viterbi decoding as *method 1* whilst that with soft demapping (12) will be referred to as *method 2*. Table I shows the bit metrics for the two methods, which are used by the VA to calculate the cumulative path metrics along the trellis.

	Method 1	Method 2
Bit metric (decoded '0')	m_0	$\left[\frac{1}{4}(m_0 - m_1) + 1\right]^2$
Bit metric (decoded '1')	m_1	$\left[\frac{1}{4}(m_0 - m_1) - 1\right]^2$

TABLE I

COMPARISON BETWEEN BIT METRIC INCREMENTS USED BY THE TWO SOFT DECODING METHODS. m_c FOR $c = 0, 1$ IS GIVEN BY (6).

Note that the difference between the bit metrics for the decoded '0' and '1' is the same for the two methods, namely $(m_0 - m_1)$.

Let $\widehat{\mathbf{b}}$ be the decoded sequence chosen by the VA with *method 1*, then its path metric is the smallest with reference to *method 1*, i.e. $M^{(1)}(\widehat{\mathbf{b}}) = M^{(1)}_{min}$. We want to demonstrate that $\widehat{\mathbf{b}}$ is also the decoded sequence obtained with *method 2*, that is $M^{(2)}(\widehat{\mathbf{b}}) = M^{(2)}_{min}$.

Assume that the decoded sequence by *method 2* is $\widehat{\mathbf{b}}' \neq \widehat{\mathbf{b}}$ and then $M^{(2)}(\widehat{\mathbf{b}}') < M^{(2)}(\widehat{\mathbf{b}})$. Because the difference between the bit metrics relative to decoded '0' and '1' is the same with both methods, it follows that also the difference between the overall metrics of two generic paths in the trellis is the same, and then

$$M^{(1)}(\widehat{\mathbf{b}}') - M^{(1)}(\widehat{\mathbf{b}}) = M^{(2)}(\widehat{\mathbf{b}}') - M^{(2)}(\widehat{\mathbf{b}}) < 0 . \quad (26)$$

Therefore $M^{(1)}(\widehat{\mathbf{b}}') < M^{(1)}(\widehat{\mathbf{b}})$, which is in contrast with the hypothesis that $\widehat{\mathbf{b}}$ is the path with the smallest cumulative sum of bit metrics for *method 1*. We can conclude that the VA always selects the same decoded bit sequence with either method.

REFERENCES

[1] ETSI TS 101 475, "Broadband Radio Access Networks (BRAN); HIPERLAN Type 2; Physical (PHY) layer, v1.2.2", 2001.

[2] R. Pyndiah, A. Picard and A. Glavieux, "Performance of Block Turbo Coded 16-QAM and 64-QAM Modulations," in *Proc. of IEEE GLOBECOM '95*, pp. 1039-43, Singapore, Nov. 1995.

[3] G. Caire, G. Taricco and E. Biglieri, "Bit-Interleaved Coded Modulation," *IEEE Trans. on Inf. Theory*, vol. 44, pp. 927-946, May 1998.

[4] X. Li and J.A. Ritcey, "Bit-Interleaved Coded Modulation with Iterative Decoding," in *Proc. of IEEE ICC '99*, pp. 858-63, June 1999.

[5] E. Zehavi, "8-PSK Trellis Codes for a Rayleigh Channel," *IEEE Trans. on Comm.*, vol. 40, pp. 873-884, May 1992.

[6] M. Speth, A. Senst and H. Meyr, "Low Complexity Space-Frequency MLSE for Multi-User COFDM," in *Proc. of IEEE GLOBECOM '99*, pp. 2395-99, Dec. 1999.

[7] A. Doufexi, S. Armour, A. Nix and D. Bull, "A Comparison of HIPERLAN/2 and IEEE.11a Phisical and MAC Layers," VTC'2000.